

# Immobilization of chitosan film containing semaphorin 3A onto a microarc oxidized titanium implant surface via silane reaction to improve MG63 osteogenic differentiation

Kaixiu Fang<sup>1,\*</sup>Wen Song<sup>2,\*</sup>Lifeng Wang<sup>1</sup>Sen Jia<sup>3</sup>Hongbo Wei<sup>1</sup>Shuai Ren<sup>1</sup>Xiaoru Xu<sup>1</sup>Yingliang Song<sup>1</sup>

<sup>1</sup>State Key Laboratory of Military Stomatology, Department of Implant Dentistry, School of Stomatology, Fourth Military Medical University, Xi'an, People's Republic of China;

<sup>2</sup>State Key Laboratory of Military Stomatology, Department of Prosthetic Dentistry, School of Stomatology, Fourth Military Medical University, Xi'an, People's Republic of China;

<sup>3</sup>State Key Laboratory of Military Stomatology, Department of Oral and Maxillofacial Surgery, School of Stomatology, Fourth Military Medical University, Xi'an, People's Republic of China

\*These authors contributed equally to this work

Correspondence: Yingliang Song  
Department of Implant Dentistry, School of Stomatology, Fourth Military Medical University, 145 West Changle Road, Xi'an 710032, People's Republic of China  
Email songyingliang@yahoo.com

**Abstract:** Improving osseointegration of extensively used titanium (Ti) implants still remains a main theme in implantology. Recently, grafting biomolecules onto a Ti surface has attracted more attention due to their direct participation in the osseointegration process around the implant. Semaphorin 3A (Sema3A) is a new proven osteoprotection molecule and is considered to be a promising therapeutic agent in bone diseases, but how to immobilize the protein onto a Ti surface to acquire a long-term effect is poorly defined. In our study, we tried to use chitosan to wrap Sema3A (CS/Sema) and connect to the microarc oxidized Ti surface via silane glutaraldehyde coupling. The microarc oxidation could formulate porous topography on a Ti surface, and the covalently bonded coating was homogeneously covered on the ridges between the pores without significant influence on the original topography. A burst release of Sema3A was observed in the first few days in phosphate-buffered saline and could be maintained for >2 weeks. Coating in phosphate-buffered saline containing lysozyme was similar, but the release rate was much more rapid. The coating did not significantly affect cellular adhesion, viability, or cytoskeleton arrangement, but the osteogenic-related gene expression was dramatically increased and calcium deposition was also abundantly detected. In conclusion, covalent bonding of CS/Sema could strongly improve osteogenic differentiation of osteoblasts and might be applied for Ti implant surface biofunctionalization.

**Keywords:** titanium, semaphorin 3A, silane reaction, microarc oxidation, osteogenic differentiation

## Introduction

Titanium (Ti) implants have been extensively used in clinics as excellent biomaterials in orthopedic and dental applications.<sup>1</sup> Despite the superb biocompatibility of Ti and the high success rate in practice,<sup>2</sup> poor osseointegration still exists in many cases, particularly in bad bone conditions such as osteoporosis or diabetes where it is difficult to establish rigid osseointegration without additional help.<sup>3</sup> Tremendous efforts have been devoted to surface modification of Ti implants to improve the osteogenic induction, and the conventional techniques mainly focus on optimizing the topography, such as the hybrid micro/nanorod topography,<sup>4</sup> or the inorganic element coating, such as strontium.<sup>4,5</sup> Unfortunately, conventional modifications are limited, and initiated osteoinductive coatings are sought. Currently, a biomimetic approach to incorporate organic bioactive molecules onto a Ti surface to activate the surface has attracted more and more attention,<sup>6</sup> among biomimetic approach immobilization of extracellular matrix

(ECM) components,<sup>7</sup> RGD-containing oligopeptide,<sup>8</sup> and growth factors<sup>9–11</sup> are mostly elucidated. The biomolecules incorporated on the Ti surface could directly intervene and participate in the natural bone healing around the implant, and consequently greatly improve Ti biofunction. More recently, semaphorin 3A (Sema3A), a diffusible axonal chemorepellent that has an important role in axon guidance, has been found to play a vital role in bone metabolism that could simultaneously promote osteoblast differentiation and inhibit osteoclast activity, and is considered to be a promising new therapeutic agent in bone diseases.<sup>12,13</sup> Therefore, Sema3A might be an optimal choice for Ti surface activation as well.

The aim of protein–implant incorporation is to pursue a simple and convenient method that could maintain the protein activity without apparent cytotoxicity and release in a controlled fashion. Chitosan is a natural cationic polymer with wonderful biocompatibility and has been used extensively for drug and nucleic acid delivery.<sup>14</sup> Chitosan film has been used as a protein carrier and for release in a sustained manner.<sup>15</sup> In addition, its amine groups could be covalently bonded to the hydroxyl group via silane glutaraldehyde coupling, which has been greatly explored to improve Ti surface bioactivity as well as antibiotic drug delivery, due to the simple procedure and strong binding strength on a Ti surface compared with a conventional adsorption process.<sup>16–18</sup> Hence, we hypothesize that chitosan film might also be an ideal carrier of Sema3A to formulate osteoinductive Ti coating via covalent bonding.

In the present study, the Ti substrate is pretreated by microarc oxidation (MAO), which is favorable for apatite deposition and osteoblast behavior,<sup>19</sup> and the surface is hydroxyl abundant after ultraviolet (UV) irradiation.<sup>20</sup> Chitosan is used to wrap Sema3A and covalently immobilize onto a UV-irradiated MAO Ti surface via silane reaction. The aim of the study is to fabricate a functional implant coating that could sustainably provide Sema3A for enhanced osseointegration.

## Materials and methods

### Materials

The pure Ti disc (diameter =1.5 cm, thickness =2 mm) was provided by the Northwest Institute for Nonferrous Metal Research (People's Republic of China). Chitosan (molecular weight 100–300 kDa, degree of deacetylation 93.37%) and 3-(4,5-dimethylthiazol-2-yl)-2,5-diphenyltetrazolium bromide (MTT) were bought from MP Biomedicals (California, USA). Other main chemicals, including calcium acetate,  $\beta$ -glycerophosphate disodium

salt pentahydrate, 3-aminopropyltriethoxysilane, glutaraldehyde, Triton™ X-100, Alizarin Red Solution, and lysozyme, were bought from Sigma-Aldrich (St Louis, MO, USA). Trizol reagent, 4',6-diamidino-2-phenylindole (DAPI), phosphate-buffered saline (PBS), and rhodamine phalloidin were purchased from Invitrogen (California, USA). Human osteoblast cell line MG63 was bought from American Type Culture Collection (Washington, USA). Dulbecco's Modified Eagle's Medium (DMEM), fetal bovine serum (FBS), and penicillin/streptomycin were purchased from Hyclone (Logan, Utah, USA). Recombinant human Sema3A was purchased from PeproTech (NJ, USA). Human Sema3A enzyme-linked immunosorbent assay (ELISA) kit was bought from Antibodies Online GmbH (Aachen, Germany). PrimeScript™ RT reagent kit and SYBR Premix Ex™ Taq II were purchased from TaKaRa (Shiga, Japan). The Protein Extraction Kit was bought from Beyotime (Jiangsu, People's Republic of China) and the antibodies used in Western blot analysis were purchased from Abcam (Cambridge, UK).

### Fabrication of MAO layer

A Ti disc was wet ground with SiC sandpaper from 100 to 800 grids and then ultrasonically cleaned in acetone, ethanol, and deionized water. The MAO procedure was performed as described previously.<sup>21</sup> Briefly, the Ti was anodized in the electrolyte containing  $\beta$ -glycerophosphate disodium salt pentahydrate (0.02 M) and calcium acetate monohydrate (0.2 M) at a voltage of 400 V for 5 minutes. The fabricated samples were ultrasonically cleaned with acetone, ethanol, and deionized water for 10 minutes each, dried at 60°C in air flow, and then sterilized by UV irradiation to form abundant hydroxyl.

### Immobilization of Sema3A-loaded chitosan (CS/Sema) film

The combination of Sema3A-loaded chitosan film (CS/Sema) and MAO Ti was by silane glutaraldehyde coupling, as described previously.<sup>18</sup> Briefly, MAO Ti samples were treated with 3-aminopropyltriethoxysilane solution (2% v/v in 95% ethanol, pH 4.5) at room temperature and rinsed with absolute ethanol. Glutaraldehyde linker (2% v/v in double distilled H<sub>2</sub>O (ddH<sub>2</sub>O), pH 4.3) was introduced to the amino end of the aminosilane to provide a reactive aldehyde group. Chitosan solution was prepared in 0.2 M acetate buffer (pH 5.5) at a concentration of 10 mg/mL and, afterwards, 3 mg Sema3A (300  $\mu$ L) was added to 2 mL of the chitosan solution and stirred continuously for 30 minutes. Three hundred microliters of the CS/Sema mixture was painted onto each MAO Ti

sample and stored at 4°C for 24 hours to allow combination with the active aldehyde group. The complex was removed and coating was neutralized by sodium hydroxide and rinsed with excess distilled water. The removed CS/Sema mixture, sodium hydroxide, and distilled water were then quantified by human Sema3A ELISA kit according to the manufacturer's instructions and subtracted from the added 300 µL. The specimen was dried by nitrogen and sterilized by ethylene oxide before cell seeding.

## Surface characterization

The specimen was critical point dried and sputter coated with platinum. The surface morphology was then observed by scanning electron microscopy (SEM, S-4800; Hitachi). Meanwhile, the water contact angle was measured by a contact angle measuring system (EasyDrop Standard; KRÜSS, Germany).

## Release profile

To simulate the release profile under physiological conditions, the samples were soaked in either 500 µL PBS or PBS containing 0.1 mg/mL lysozyme (PBS + lysozyme) under a humidified atmosphere of 5% CO<sub>2</sub> at 37°C. At predetermined time points, the supernatant was collected and replaced with fresh buffer. The elution was quantified by human Sema3A ELISA kit. The accumulated released Sema3A was calculated manually by adding each sample. In addition, the substrate morphology after dissolution in PBS at several indicated time points was also observed by SEM to understand the degradation process.

## Cell culture and seeding

The MG63 cell line was maintained in DMEM supplemented with 10% FBS containing 100 U/mL penicillin and 100 µg/mL streptomycin. Medium was changed twice a week, and when the confluence attained 80%, cells were trypsinized and centrifuged at 800 rpm for 5 minutes. The pellet was suspended with fresh medium to obtain the concentration of 2×10<sup>4</sup>/mL and 1 mL was added to each Ti sample placed in a 24-well plate.

## Cell adhesion

Cell adhesion was performed as previously reported.<sup>22</sup> Specifically, cells were seeded on the specimens and allowed to attach for 2 hours. The cells were rinsed in PBS solution to remove the nonadherent cells, followed by fixation in 4% paraformaldehyde for 15 minutes, and stained with DAPI for 10 minutes under dark conditions. After rinsing thoroughly in PBS, the samples were observed by fluorescence microscopy (Leica). Five fields of each group were randomly selected and the cell number was counted. Meanwhile, the cells were fixed

with 2% glutaraldehyde overnight and dehydrated gradually with ethanol from 30% to 100%. The specimens were sputter coated with platinum and observed by SEM.

## Cytotoxicity assay

To assess the cytotoxicity of the coating, 200 µL MTT (5 mg/mL in PBS) and 800 µL medium were mixed and added into each well at different time points. After 4 hours of incubation, the medium was gently removed and 1 mL dimethyl sulfoxide was added to dissolve the precipitation. Two hundred microliters of the solution was transferred to a new 96-well plate and the absorbance was read at 490 nm.

## Cytoskeleton staining

The cells were fixed 4 days postseeding by 4% paraformaldehyde for 15 minutes and treated with 0.1% Triton-X100 for 15 minutes. The actin filament was then stained by rhodamine phalloidin (50 µg/mL in PBS) for 1 hour and rinsed with PBS three times. The nucleus was stained with DAPI thereafter and specimens were observed by confocal laser scanning microscopy (Olympus).

## Osteogenic-related gene expression

The osteogenic induction was performed 3 days post-cell plating by osteogenic medium containing 10 mM β-glycerophosphate, 50 mg/mL ascorbic acid, and 10<sup>-7</sup> M dexamethasone. After induction for 3 and 7 days, total ribonucleic acid (RNA) was isolated by TRIzol Reagent according to the manufacturer's instructions. After quantification by optical density measurement, 1 µg total RNA underwent reverse transcription to complementary deoxyribonucleic acid (cDNA) by PrimeScript™ RT reagent kit. Normalized cDNA was used to amplify with SYBR Premix Ex™ Taq II RT-PCR kit in Applied Biosystems 7,500 Real-Time PCR System. The related primers sequences were designed according to a published article<sup>23</sup> and are listed in Table 1. The messenger RNA expression was calculated based on the Ct value, defined as the cycle number when the fluorescence reaches a threshold, and β-actin was used as an endogenous reference.

## Western blot analysis

The osteogenic proteins were analyzed by Western blot after 3 days of induction. Briefly, total protein was extracted using a Protein Extraction Kit (Beyotime), according to the manufacturer's instructions. The protein concentration was measured using a BCA protein assay kit (Beyotime). The proteins were separated by 10% sodium dodecyl sulfate polyacrylamide gel electrophoresis and blotted on 0.45 µm polyvinylidene fluoride membrane (Pall Corporation, USA). After blocking with bovine

**Table 1** Primers used for real-time quantitative polymerase chain reaction

Gene	Forward primer sequence (5'-3')	Reverse primer sequence (5'-3')
RUNX2	CACTGGCGCTGCAACAAGA	CATTCCGGAGCTCAGCAGAATAA
ALP	CCTTGTAGCCAGGCCATTG	GGACCATTCCCACGTCTTCAC
OCN	CCCAGGCGCTACCTGTATCAA	GGTCAGCCAACCTCGTCACAGTC
BMP	CAACACCGTGCTCAGCTTCC	TTCCCACTCATTTCTGAAAGTTCC
$\beta$ -actin	TGGCACCCAGCACAATGAA	CTAAGTCATAGTCCGCCTAGAAGCA

**Abbreviations:** RUNX2, runt-related transcription factor 2; ALP, alkaline phosphatase; OCN, osteocalcin; BMP, bone morphogenetic protein.

serum albumin for 1 hour, the membrane was incubated with human monoclonal antibody overnight. After extensive washes, the immunodetection was performed using the enhanced chemoluminescence reagent (Santa Cruz, USA).

## ECM mineralization

The cells were osteogenically induced for 21 days and fixed in 2.5% glutaraldehyde (freshly prepared in PBS) for 15 minutes at room temperature. Then, the calcium deposition in ECM was stained by Alizarin Red Solution (40 mM in distilled H<sub>2</sub>O (dH<sub>2</sub>O), pH 4.2) for 5 minutes, followed by plenty of distilled water rinsing to remove any excess dye. Images were taken and analyzed by stereomicroscope (Leica). Meanwhile, the stained nodules were stripped by 10% (w/v) cetylpyridinium chloride solution and the absorbance was measured at 620 nm.

## Statistical analysis

The three independent experiments were replicated and results were presented as mean  $\pm$  standard error. One-way analysis of variance and the Student–Newman–Keuls post hoc test were performed to compare the difference, and  $P < 0.05$  was considered significant.

## Results

### Surface characterization

Multipores ranging from 1 to 5  $\mu$ m were observed on a Ti surface after MAO treatment and the surface of the ridges was smooth (Figure 1A). When the MAO surface was coated with CS/Sema, the multipores still existed without significant change; however, the ridges were apparently covered by a homogeneous coating (Figure 1A). The MAO-treated Ti was hydrophilic with the water contact angle of  $\sim 10^\circ$ , whereas it increased substantially to  $\sim 80^\circ$  after CS/Sema coating (Figure 1B).

### Release profile

The release profile was carried out in PBS or PBS + lysozyme and the released Sema3A was quantified based on the ELISA

kit by absorbance measurement after being incorporated with Sema3A antibody (Figure 2A). The substrate morphology was also observed by SEM after 1, 3, 7, and 14 days of incubation in PBS (Figure 2B). In the quantification test, a burst release was observed during the first 3 days when approximately 60% was released, and the rate slowed down afterwards in PBS (Figure 1A). However, once the coating was soaked in PBS + lysozyme, the release rate was substantially speeded up so that  $>80\%$  was released during the initial 2 days and was nearly dissolved entirely after 5 days (Figure 2A). In the morphology observation, the surface coating was slightly rough and no particular coating morphology change was observed at day 1 (Figure 2B [B1]). At day 3, the homogeneous coating was collapsed and replaced by numerous particles and debris (Figure 2B [B2]). One week later, the debris had mostly decreased (Figure 2B [B3]) and the surface became clear and clean eventually at day 14 (Figure 2B [B4]), which means that the coating was almost totally degraded.

### Cell adhesion

Cell number attached on different coatings was shown by DAPI staining (Figure 3A). It seemed that the number on

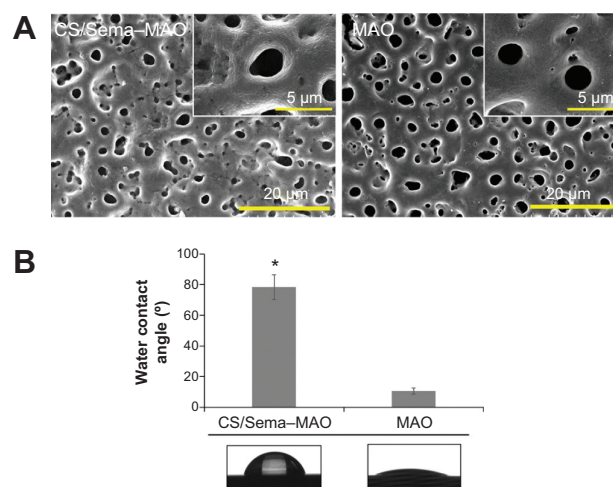


**Figure 1** The coating morphology observation by scanning electron microscopy (A) and water contact angle measurement (B).

**Note:** \* $P < 0.05$  vs MAO.

**Abbreviations:** CS/Sema, chitosan–semaphorin 3A; MAO, microarc oxidation.

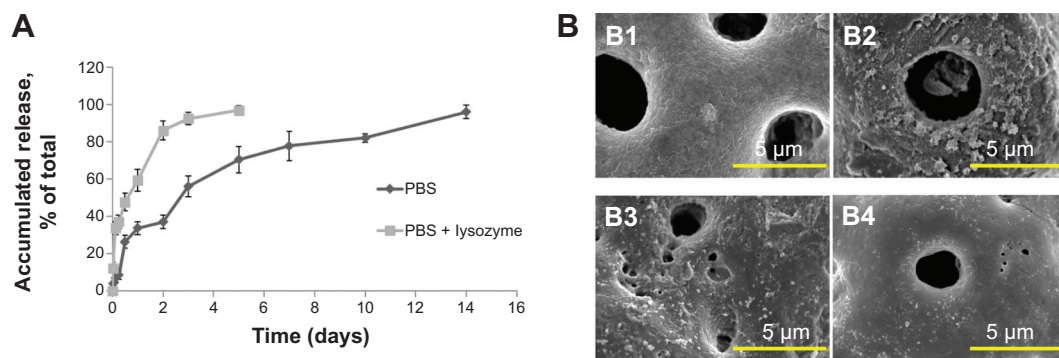


**Figure 2** Accumulated release profile of CS/Sema-MAO in PBS and PBS + lysozyme (**A**) and the morphology observation of the substrate after 1 day (**B1**), 3 days (**B2**), 7 days (**B3**), and 14 days (**B4**) of dissolution in PBS.

**Abbreviations:** CS/Sema, chitosan–semaphorin 3A; MAO, microarc oxidation; PBS, phosphate-buffered saline.

CS/Sema-MAO and CS/BSA-MAO was slightly more than CS-MAO or MAO, but there was no statistical significance between all the groups (Figure 3C). The SEM images revealed that the adhered cells exhibited topographically dependent morphogenesis and the pseudopodia were established on all the groups (Figure 3B).

### Cytotoxicity assay

The cytotoxicity was evaluated by cell viability assessment. More than 80% cell viability without significant difference

was observed on all the coatings at day 1 (Figure 4). Thereafter, it mildly changed at day 3 and day 7, but still no significant difference was observed compared with control groups (Figure 4).

### Actin filaments arrangement

Immunofluorescence assay was performed to exhibit the cytoskeleton. It revealed that the cytoskeleton was not significantly affected and cells spread out well on all the groups (Figure 5). Cell–cell connection had been well established

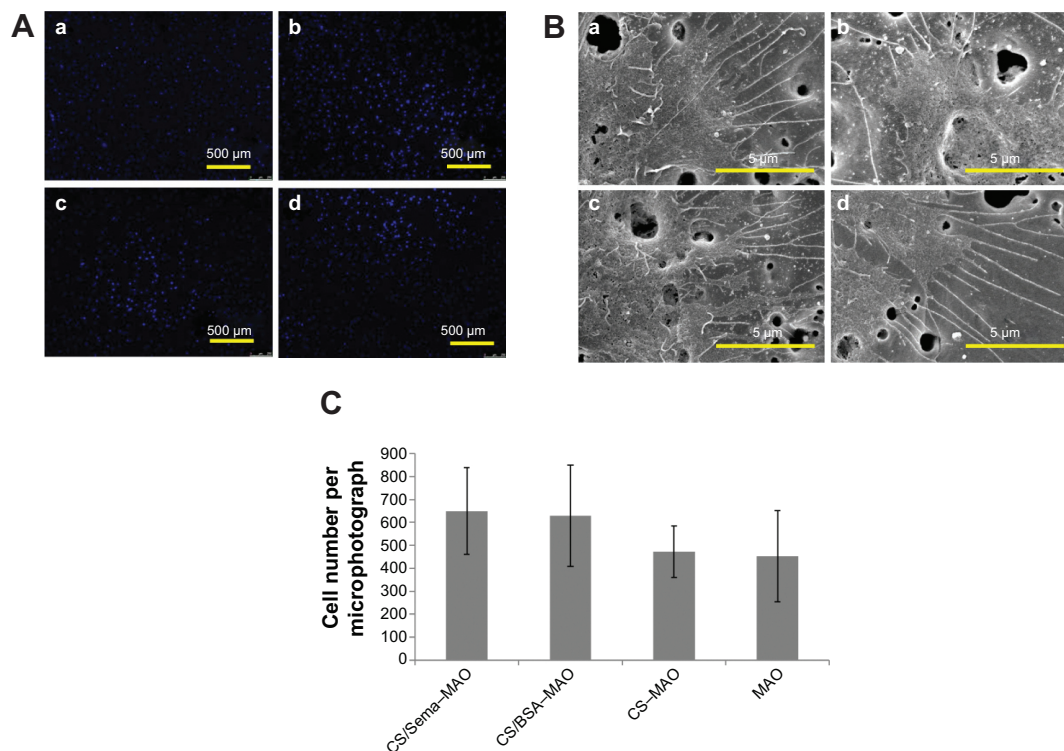


**Figure 3** Cell adhesion visualized by 4',6-diamidino-2-phenylindole staining (**A**), scanning electron microscope (**B**) and number counts (**C**).

**Notes:** (A)(a) and (B)(a): CS/Sema-MAO; (A)(b) and (B)(b): CS/BSA-MAO; (A)(c) and (B)(c): CS-MAO; (A)(d) and (B)(d): MAO.

**Abbreviations:** CS/Sema, chitosan–semaphorin 3A; MAO, microarc oxidation; CS/BSA, chitosan-bovine serum albumin.

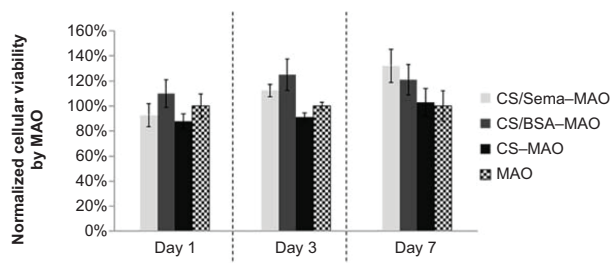


**Figure 4** Cellular viability carried out by 3-(4,5-dimethylthiazol-2-yl)-2, 5-diphenyltetrazolium bromide assay.

**Abbreviations:** CS/Sema, chitosan–semaphorin 3A; MAO, microarc oxidation; CS/BSA, chitosan–bovine serum albumin.

on all the substrates and the actin filaments seemed more noticeable at the cell edges, particularly on the MAO surface (Figure 5).

### Osteogenic-related gene and protein expression

The osteogenic-related genes of runt-related transcription factor 2 (*RUNX2*), alkaline phosphatase (*ALP*), osteocalcin (*OCN*), and bone morphogenetic protein (*BMP*) were measured by real-time quantitative polymerase chain reaction (qPCR) at day 3 and day 7 separately. All the related genes determined in our study were elevated on a CS/Sema–MAO surface compared with control groups in general (Figure 6).

Specifically, *RUNX2* was increased over three-fold and *ALP*, *OCN*, and *BMP* over two-fold on CS/Sema–MAO compared with control groups at day 3 (Figure 6A). Afterwards, on day 7, *RUNX2* returned to normal levels whereas *ALP* and *BMP* were over three-fold and *OCN* over two-fold (Figure 6B). No significant difference was observed on CS/BSA–MAO or CS–MAO in any time points. The counter protein expression at day 3 was analyzed. In agreement with the qPCR measurement, all the detected osteogenic proteins were enormously upregulated on a CS/Sema–MAO surface (Figure 6C).

### ECM mineralization

The osteogenic differentiation was further confirmed by Alizarin Red Solution staining after osteogenic induction for 21 days (Figure 7). The area of ECM mineralization nodules on a CS/Sema–MAO surface was significantly larger and denser than control groups (Figure 7A). The CS/BSA–MAO or CS–MAO mineralization seemed slightly more robust than naked MAO (Figure 7A) and the semiquantification assay also confirmed it (Figure 7B).

### Discussion

Grafting biomolecules onto Ti implants is considered to be a pivotal approach to promote osseointegration, and the

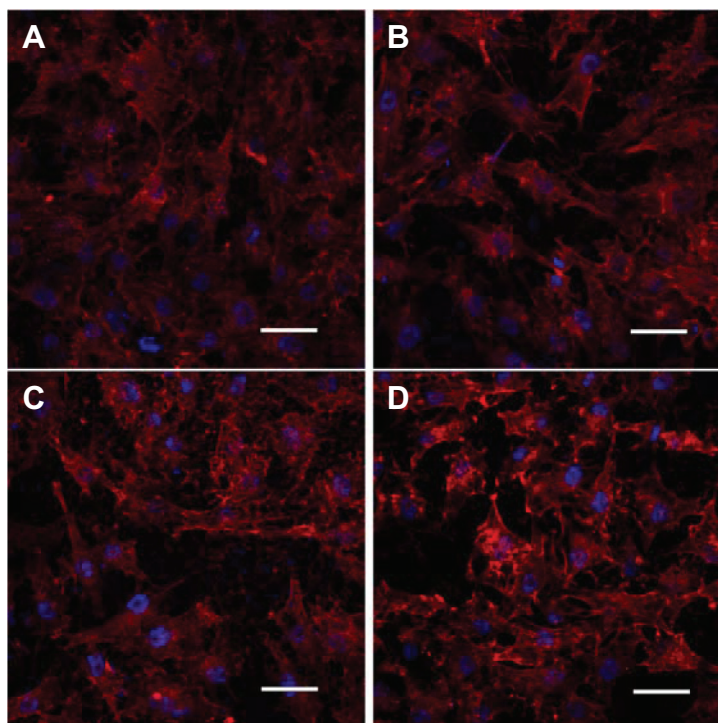


**Figure 5** Cytoskeleton staining by rhodamine phalloidin under confocal laser scanning microscopy observation.

**Notes:** A: CS/Sema–MAO; B: CS/BSA–MAO; C: CS–MAO; D: MAO; scale bar = 100  $\mu$ m.

**Abbreviations:** CS/Sema, chitosan–semaphorin 3A; MAO, microarc oxidation.

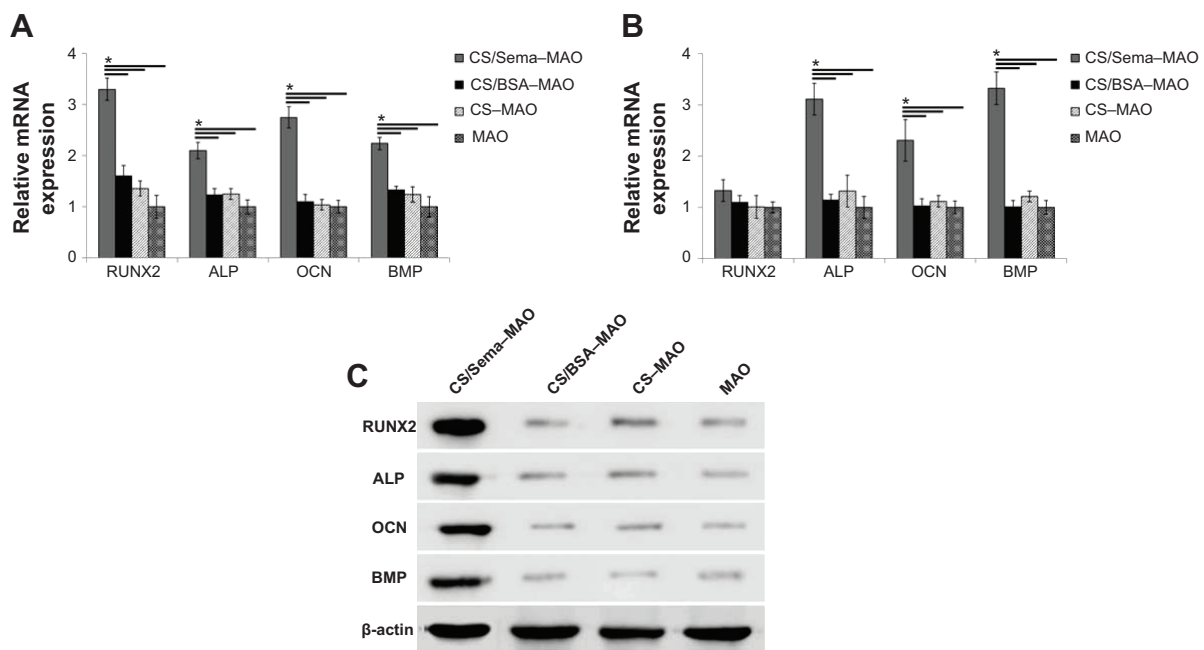


**Figure 6** Osteogenic-related gene expression quantified by real-time quantitative polymerase chain reaction after osteogenic induction of 3 days (A) and 7 days (B). The relative protein level after 3 days of culture was analyzed with Western blot (C).

**Notes:** \* $P < 0.05$  vs CS/BSA-MAO, CS-MAO, and MAO.

**Abbreviations:** CS/Sema, chitosan–semaphorin 3A; MAO, microarc oxidation; RUNX2, runt-related transcription factor 2; ALP, alkaline phosphatase; OCN, osteocalcin; BMP, bone morphogenetic protein; CS/BSA, chitosan-bovine serum albumin; mRNA, messenger RNA.

novel Sema3A protein has been chosen in our biofunctionalization study. In order to immobilize the protein onto a Ti surface, silane reaction is selected due to the rigid covalent bond that could sustainably provide the protein as well as the convenient treating procedure. Sema3A was loaded in chitosan solution and the abundant amine groups in chitosan could perfectly combine with hydroxyl groups produced by MAO treatment and UV irradiation.<sup>20</sup> The morphology

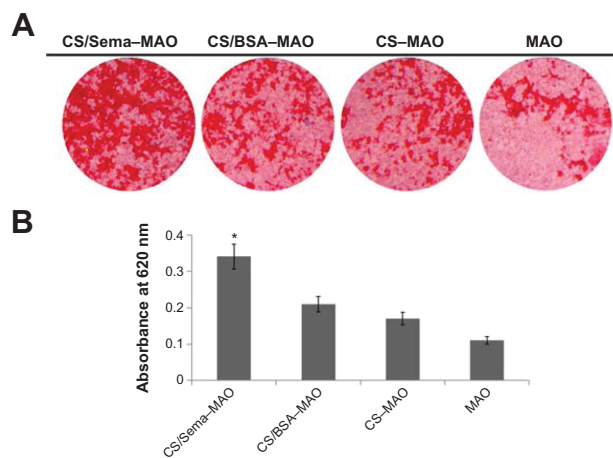


**Figure 7** Extracellular matrix mineralization stained by Alizarin Red Solution (A) and optical density measurement (B).

**Notes:** \* $P < 0.05$  vs CS/BSA-MAO, CS-MAO, and MAO.

**Abbreviations:** CS/Sema, chitosan–semaphorin 3A; MAO, microarc oxidation; CS/BSA, chitosan-bovine serum albumin.

observation revealed that the MAO treatment could formulate a porous multipore topography due to the occurrence of discharges under high potentials<sup>23</sup> and abundant hydroxyl groups that result in hydrophilic surface.<sup>24</sup> The following silane reaction could formulate a homogeneous coating on the surface without influencing MAO pores, which guaranteed the original MAO topography. The modified implant had an extremely higher water contact angle compared with naked MAO, which might be attributed to the hydrophobic property of chitosan.<sup>25</sup> In the release profile, even though the burst release existed in the first few days, the covalent bond coating could maintain Sema3A for 2 weeks in PBS, which was longer than the antimicrobial release described previously.<sup>17</sup> The difference might be explained by the fact that, not only the amine groups of chitosan but also of Sema3A have been covalently bonded to the active aldehyde groups during coating formulation. The release rate in lysozyme was much faster, which should be attributed to the degradation caused by lysozyme.<sup>26</sup>

Although many reports hold the idea that chitosan film could improve cell adhesion and proliferation,<sup>16,27</sup> there are also conflicts that there is no significant cell growth improvement.<sup>26,28</sup> Our result is in agreement with the latter that no significant difference of attachment and viability has been observed between CS-MAO and MAO, and because

Sema3A has no dramatic influence on cellular viability and proliferation,<sup>13</sup> CS/Sema-MAO has not shown enhancement of cell growth either. Anyway, it indicates that our coating has favorable biocompatibility without obvious cytotoxicity. It is also considered that Sema3A regulates actin cytoskeletal rearrangement,<sup>29,30</sup> but no particular actin filament alteration has been detected on our CS/Sema-MAO coatings. The problem might possibly be put down to that the culture duration is different and the pattern of Sema3A treatment in our study is the reverse from the substrate coating, which might also be different from adding directly into culture medium. The osteogenic differentiation assay proved that a Sema3A-incorporated implant could enormously improve osteogenic marked gene and protein expression and ECM mineralization. It has been elucidated that the binding of Sema3A and neuropilin-1 can stimulate osteoblast differentiation through the canonical Wnt/ $\beta$ -catenin signaling pathway and, in addition, the binding can also inhibit receptor activator of nuclear factor- $\kappa$ B ligand-induced osteoclast differentiation by inhibiting the immunoreceptor tyrosine-based activation motif and RhoA signaling pathways.<sup>13</sup> Consequently, Sema3A can be used as a powerful osteogenic promotion agent. Since the silane reaction is a handy method to combine chitosan and Ti, and chitosan is also an ideal drug reservoir, our study might not be limited only to protein immobilization but could be used for other drug coatings.

## Conclusion

We have immobilized a novel osteoprotection protein Sema3A onto an MAO-treated Ti surface with the assistance of chitosan via silane glutaraldehyde coupling. The immobilized coating is homogeneously covered on a ridged surface without blocking the pores formulated by MAO under SEM observation and could maintain Sema3A for ~2 weeks. It has no particular influence on MG63 cellular attachment, viability, or cytoskeleton arrangement but could promote osteogenic differentiation tremendously. The study offers a meaningful Ti implant biofunctionalization technique and is also referential for other molecule delivery from an implant surface.

## Acknowledgments

The work is supported by grants from the Nature Science Foundation of China (NSFC Nos. 81170984 and 81300918). The authors appreciate the grants from the School of Stomatology, Fourth Military Medical University.

## Disclosure

The authors declare no conflicts of interest relevant to this work.

## References

- Elias CN, Lima JHC, Valiev R, Meyers MA. Biomedical applications of titanium and its alloys. *JOM*. 2008;60(3):46–49.
- Buser D, Janner SF, Wittneben JG, Bragger U, Ramseier CA, Salvi GE. 10-year survival and success rates of 511 titanium implants with a sandblasted and acid-etched surface: a retrospective study in 303 partially edentulous patients. *Clin Implant Dent Relat Res*. 2012; 14(6):839–851.
- Zhou X, Zhang P, Zhang C, Zhu Z. Promotion of bone formation by naringin in a titanium particle-induced diabetic murine calvarial osteolysis model. *J Orthop Res*. 2010;28(4):451–456.
- Zhang W, Li Z, Huang Q, et al. Effects of a hybrid micro/nanorod topography-modified titanium implant on adhesion and osteogenic differentiation in rat bone marrow mesenchymal stem cells. *Int J Nanomedicine*. 2013;8:257–265.
- Li Y, Feng G, Gao Y, Luo E, Liu X, Hu J. Strontium ranelate treatment enhances hydroxyapatite-coated titanium screws fixation in osteoporotic rats. *J Orthop Res*. 2010;28(5):578–582.
- Kim TI, Jang JH, Kim HW, Knowles JC, Ku Y. Biomimetic approach to dental implants. *Curr Pharm Des*. 2008;14(22):2201–2211.
- Morra M. Biochemical modification of titanium surfaces: peptides and ECM proteins. *Eur Cell Mater*. 2006;12:1–15.
- Kim T-I, Lee G, Jang J-H, Chung C-P, Ku Y. Influence of RGD-containing oligopeptide-coated surface on bone formation in vitro and in vivo. *Biotechnol Lett*. 2007;29(3):359–363.
- Wang F, Song YL, Li CX, et al. Sustained release of insulin-like growth factor-1 from poly(lactide-co-glycolide) microspheres improves osseointegration of dental implants in type 2 diabetic rats. *Eur J Pharmacol*. 2010;640(1–3):226–232.
- Liu Y, Enggist L, Kuffer AF, Buser D, Hunziker EB. The influence of BMP-2 and its mode of delivery on the osteoconductivity of implant surfaces during the early phase of osseointegration. *Biomaterials*. 2007; 28(16):2677–2686.
- Shimono K, Oshima M, Arakawa H, Kimura A, Nawachi K, Kuboki T. The effect of growth factors for bone augmentation to enable dental implant placement: a systematic review. *Jpn Dent Sci Rev*. 2010;46(1): 43–53.
- Fukuda T, Takeda S, Xu R, et al. Sema3A regulates bone-mass accrual through sensory innervations. *Nature*. 2013;497:490–493.
- Hayashi M, Nakashima T, Taniguchi M, Kodama T, Kumanogoh A, Takayanagi H. Osteoprotection by semaphorin 3A. *Nature*. 2012; 485(7396):69–74.
- Rudzinski WE, Aminabhavi TM. Chitosan as a carrier for targeted delivery of small interfering RNA. *Int J Pharm*. 2010;399(1–2):1–11.
- Abarrategi A, Civantos A, Ramos V, Sanz Casado JV, López-Lacomba JL. Chitosan film as rhBMP2 carrier: delivery properties for bone tissue application. *Biomacromolecules*. 2007;9(2):711–718.
- Renoud P, Toury B, Benayoun S, Attik G, Grosgeat B. Functionalization of titanium with chitosan via silanation: evaluation of biological and mechanical performances. *PLoS ONE*. 2012;7(7):e39367.
- Norowski PA, Courtney HS, Babu J, Haggard WO, Bumgardner JD. Chitosan coatings deliver antimicrobials from titanium implants: a preliminary study. *Implant Dent*. 2011;20(1):56–67.
- Swanson TE, Cheng X, Friedrich C. Development of chitosan-vancomycin antimicrobial coatings on titanium implants. *J Biomed Mater Res A*. 2011; 97(2):167–176.
- Huang P, Zhang Y, Xu K, Han Y. Surface modification of titanium implant by microarc oxidation and hydrothermal treatment. *J Biomed Mater Res B Appl Biomater*. 2004;70B(2):187–190.
- Han Y, Chen D, Sun J, Zhang Y, Xu K. UV-enhanced bioactivity and cell response of micro-arc oxidized titania coatings. *Acta Biomater*. 2008;4(5):1518–1529.
- Song W, Wu K, Yan J, Zhang Y, Zhao L. MiR-148b laden titanium implant promoting osteogenic differentiation of rat bone marrow mesenchymal stem cells. *RSC Adv*. 2013;3(28):11292–11300.



22. Zhao L, Mei S, Wang W, Chu PK, Wu Z, Zhang Y. The role of sterilization in the cytocompatibility of titania nanotubes. *Biomaterials*. 2010;31(8):2055–2063.
23. Wang W, Zhao L, Ma Q, Wang Q, Chu PK, Zhang Y. The role of the Wnt/beta-catenin pathway in the effect of implant topography on MG63 differentiation. *Biomaterials*. 2012;33(32):7993–8002.
24. Dunleavy CS, Golosnoy IO, Curran JA, Clyne TW. Characterisation of discharge events during plasma electrolytic oxidation. *Surf Coat Technol*. 2009;203(22):3410–3419.
25. Wang X, Xi Z, Liu Z, Yang L, Cao Y. The fabrication and property of hydrophilic and hydrophobic double functional bionic chitosan film. *J Nanosci Nanotechnol*. 2011;11(11):9737–9740.
26. Yuan Y, Chesnutt BM, Wright L, Haggard WO, Bumgardner JD. Mechanical property, degradation rate, and bone cell growth of chitosan coated titanium influenced by degree of deacetylation of chitosan. *J Biomed Mater Res B Appl Biomater*. 2008;86(1):245–252.
27. Custódio CA, Alves CM, Reis RL, Mano JF. Immobilization of fibronectin in chitosan substrates improves cell adhesion and proliferation. *J Tissue Eng Regen Med*. 2010;4(4):316–323.
28. Hamilton V, Yuan Y, Rigney DA, et al. Characterization of chitosan films and effects on fibroblast cell attachment and proliferation. *J Mater Sci Mater Med*. 2006;17(12):1373–1381.
29. Tran TS, Kolodkin AL, Bharadwaj R. Semaphorin regulation of cellular morphology. *Annu Rev Cell Dev Biol*. 2007;23:263–292.
30. Lepelletier Y, Moura IC, Hadj-Slimane R, et al. Immunosuppressive role of semaphorin-3A on T cell proliferation is mediated by inhibition of actin cytoskeleton reorganization. *Eur J Immunol*. 2006;36(7):1782–1793.

### International Journal of Nanomedicine

### Publish your work in this journal

The International Journal of Nanomedicine is an international, peer-reviewed journal focusing on the application of nanotechnology in diagnostics, therapeutics, and drug delivery systems throughout the biomedical field. This journal is indexed on PubMed Central, MedLine, CAS, SciSearch®, Current Contents®/Clinical Medicine,

Submit your manuscript here: <http://www.dovepress.com/international-journal-of-nanomedicine-journal>

Dovepress

Journal Citation Reports/Science Edition, EMBase, Scopus and the Elsevier Bibliographic databases. The manuscript management system is completely online and includes a very quick and fair peer-review system, which is all easy to use. Visit <http://www.dovepress.com/testimonials.php> to read real quotes from published authors.